U. Walzer. Melting temperature systematics of binary intermetallic compounds.
High Temp. - High Pressures, 24:35-44, 1992

High Temperatures–High Pressures, 1992, volume 24, pages 35–44

Melting temperature systematics of binary intermetallic compounds

Uwe Walzer
Institut für Geowissenschaften, Universität Jena, Burgweg 11, 6900 Jena, Germany
Received 26 June 1990

Abstract. The melting temperature of pure metals is calculated as a function of the relative volume. The calculation of pressure–temperature phase diagrams and of composition–temperature phase diagrams is discussed. The systematics of the distribution of the melting temperatures of binary metallic compounds and alloys are considered. Ion-core pseudopotentials have been derived through full-core atom calculations based on the Dirac equation and the points of minimum and the points of maximum curvature of these have been plotted as a function of the distance from the centre of the atom. The systematics evident in the plots allows a theoretical prediction of the magnitude of the melting temperatures to be made.

1 Introduction

This paper is significant for the understanding of both the metallurgy and the physics of metallic planetary cores. For the questions of the accretion mechanism of the Earth, the gravitational segregation of the core and mantle of the Earth, and the thermal regime of the Earth's core (Ullmann and Walzer 1980; Jacobs 1987), it is useful to subdivide the topic into the following partial problems:

—determination of the pressure–temperature phase diagram for one component, eg iron;

—determination of the concentration–temperature binary phase diagrams for zero pressure;

—determination of the melting temperature for an intermetallic compound or alloy with a fixed ratio of the numbers of atoms, derived from ab initio calculations and the systematics of the data that results from their arrangement in the periodic table. This is the main objective of this paper. Cosmochemical, geomagnetic, seismological, and other questions which are related to the overall topic, will not be treated in this paper.

2 Melting-point curve and pressure–temperature phase diagram

Frequent use has been made of Simon's (1937) semiempirical formula for the relationship between the melting temperature, T_m, and the pressure, P, for a uniform phase of a material:

$$\frac{P_m}{P_0} = \left(\frac{T_m}{T_0}\right)^c - 1, \tag{1}$$

where T_0 is the melting temperature at atmospheric pressure and P_0 is a pressure constant.

Gilvarry (1956) has shown that this formula can be derived from a modification of the Lindemann melting-point theory. He assumed that the mean-square value of the amplitudes of the heat oscillations must reach a certain fixed percentage of the distance between nearest neighbours. One has

$$c = \frac{(6\gamma + 1)}{(6\gamma - 2)}, \tag{2}$$

where γ is the Grüneisen parameter. The following statement generally applies: at each point of the melting-point curve, the Gibbs free energies of the solid, G_{sol},

and of the liquid, G_{liq}, must be identical. Consequently, from the first law of thermodynamics,

$$(E - T_m S + PV)_{sol} = (E - T_m S + PV)_{liq}, \tag{3}$$

where E is the internal energy, S is the entropy, and V is the volume. If the pressure along the melting-point curve changes by dP, then $dG_{sol} = dG_{liq}$ must always apply. If the total differential of G is formed and $dE - T_m dS + P dV = 0$ is substituted, one obtains the Clausius–Clapeyron equation

$$\frac{dT_m}{dP} = \frac{(V_{liq} - V_{sol})}{(S_{liq} - S_{sol})}, \tag{4}$$

or

$$\frac{d}{dP} \ln T_m = \frac{V_{liq} - V_{sol}}{L}, \tag{5}$$

where L is the latent heat of melting. The three variables on the right-hand side of equation (5) are all still dependent on the pressure. Now, in order to be able to define explicitly the dependence of the melting temperature T_m on the pressure P or on the relative volume, $x = V/V_0$, special assumptions have to be introduced. The melting temperature depressions which are observed (eg for Ge, Ga, Sb, and Bi) are related with all probability to phase transitions from loosely packed structures to more densely packed ones. However, the interest here is in very high pressures and a dense packing of spheres. In this section therefore, the Lindemann melting law is used:

$$\frac{1}{T_m}\frac{dT_m}{dP} = \frac{2(\gamma - \frac{1}{3})}{B}, \tag{6}$$

where B is the isothermal bulk modulus along the melting curve. For similar purposes, Stacey and Irvine (1977), and Stevenson (1980) derived formulas for the melting points. These formulas differ only slightly from the Lindemann law. To calculate γ I use the free volume theory of Vashchenko and Zubarev (1963). This theory can also be derived from the assumption of purely central forces between the atoms—with no special assumptions about the form of the interatomic potential being required. γ is given by

$$\gamma = \left(\frac{1}{2}\frac{dB}{dP} - \frac{5}{6} + \frac{2}{9}\frac{P}{B}\right)\left(1 - \frac{4}{3}\frac{P}{B}\right)^{-1}. \tag{7}$$

Since $B = -x\,dP/dx$, the only thing that is still required is an approximation of the equation of state favourable for dense atom packings. I take model 1 of Ullmann and Pan'kov (1976), which was found to be suitable compared with other models suggested (Walzer et al 1979):

$$P = -\frac{3B_0}{2 - B_1}\left[x^{(1-2B_1)/3} - x^{-(1+B_1)/3}\right]. \tag{8}$$

B_0 denotes the zero pressure bulk modulus and B_1 is the first derivative of the bulk modulus with pressure at $P = 0$. From equation (6),

$$\frac{d \ln T_m}{d \ln x} = 2\left(\frac{1}{3} - \gamma\right). \tag{9}$$

By use of the substitutions $T_m = e^{\tau}$ and $x = e^{\xi}$, it is possible to exactly solve this differential equation to give:

$$\tau(\xi) = \frac{2 - B_1}{3}\xi + \ln\left\{\frac{2B_1 - 5}{B_1 - 3}\exp\left[\frac{(2 - B_1)}{3}\xi\right] - 1\right\} + \text{constant}. \tag{10}$$

From this follows the relationship between the melting temperature and the relative volume x:

$$\frac{T_m}{T_{m,0}} = \frac{2B_1 - 5}{B_1 - 3} x^{(4-2B_1)/3} - x^{(2-B_1)/3}. \tag{11}$$

Walzer (1983) derived this formula using a completely different approach, namely a dislocation model and an interatomic pair potential. Poirier (1986) also used a dislocation model for melting in the geophysical field. Equation (11) has proven its worth for modelling the melting of crystals that have a dense packing of spheres; in every case, the experimental values are well approximated. In analogy with the Leibfried number or the Bragg number, one forms a dimensionless quantity Q_0:

$$Q_0 = \frac{R_0 T_m \rho}{(F_0 B)}, \tag{12}$$

where R_0 is the universal gas constant, ρ is the density, and F_0 is the formula weight. If the bulk modulus is plotted as a function of the melting temperature, one observes quite unsystematic clouds of points at low pressures, but a linear relationship at high pressures. Figure 1 shows a plot of Q_0 as a function of P, the formulae of this section

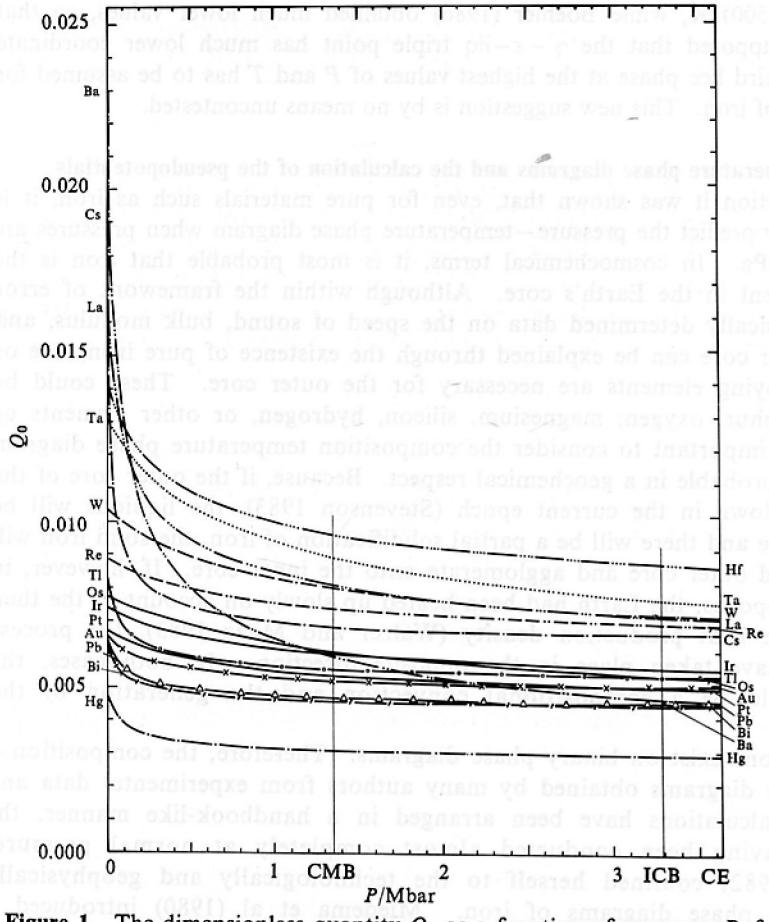

Figure 1. The dimensionless quantity Q_0 as a function of pressure, P, for the elements of the sixth period. CMB corresponds to the pressure at the core–mantle boundary of the Earth, ICB to the pressure at the inner core boundary, and CE to the pressure at the centre of the Earth.

having been substituted in equation (12). For the purpose of clarity, only the elements of the sixth period are shown. Two bundles of curves are found for high pressures. The lower bundle essentially comprises elements which already have fcc and hcp lattices at normal pressure. If one assumes the densest packing of spheres for the Earth's core—that is, for the region to the right of the vertical line CMB—one can estimate T_m/F_0 without knowing the chemical composition. This is so because, from geophysics, ρ and B are quite well known as functions of pressure and depth, respectively. Meanwhile, for d-state metals, equation (8) can be replaced by a better approximation. From a combination of the pseudopotential theory and muffin-tin orbital theory, the total energy per ion, the equation of state, bulk modulus and its derivatives, can be predicted in a practicable manner (Walzer 1987a, 1987b). It should be emphasised again that the melting-point theory used here is tied to the existence of the densest packing of spheres on the crystalline side of the curve.

With respect to the appropriate pressure–temperature phase diagram for iron, there is no consensus among authors for the high-pressure range. For 330 GPa—ie for the pressure on the inner-core boundary of the Earth—Brown and McQueen (1982), using shock-wave experiments, measured a melting point of iron at (6200 $\pm$ 500) K, whereas estimates based on the Lindemann law yield 7850 K. With the help of extrapolations of static experiments with a laser-heated diamond cell, Williams et al (1987) arrived at a value of (7600 $\pm$ 500) K, while Boehler (1986) obtained much lower values, so that Anderson (1989) supposed that the $\gamma-\varepsilon-$liq triple point has much lower coordinate values and that a third bcc phase at the highest values of P and T has to be assumed for the phase diagram of iron. This new suggestion is by no means uncontested.

3 Composition temperature phase diagrams and the calculation of the pseudopotentials

In the previous section it was shown that, even for pure materials such as iron, it is difficult to correctly predict the pressure–temperature phase diagram when pressures are higher than 100 GPa. In cosmochemical terms, it is most probable that iron is the dominant component in the Earth's core. Although within the framework of error limits, the geophysically determined data on the speed of sound, bulk modulus, and density in the inner core can be explained through the existence of pure iron, one or several lighter alloying elements are necessary for the outer core. These could be admixtures of sulphur, oxygen, magnesium, silicon, hydrogen, or other elements or compounds. It is important to consider the composition temperature phase diagram of alloys that are probable in a geochemical respect. Because, if the outer core of the Earth is cooling down in the current epoch (Stevenson 1983), the liquidus will be reached from above and there will be a partial solidification of iron, the solid iron will sink into the liquid outer core and agglomerate onto the inner core. If, however, in earlier geological epochs, the Earth had been heated up slowly on account of the then greater radioactive heat production density (Walzer and Maaz 1983), the process would formerly have taken place in the opposite direction. In both cases, the consequence would be a compositional convection and the generation of the geomagnetic field.

Many publications exist on binary phase diagrams. Therefore, the composition–temperature phase diagrams obtained by many authors from experimental data and thermochemical calculations have been arranged in a handbook-like manner, the measurements having been conducted almost completely at normal pressure. Kubaschewski (1982) confined herself to the technologically and geophysically significant binary phase diagrams of iron. Miedema et al (1980) introduced a semiempirical model of alloy cohesion. This model assigns only two coordinates to each element: the average of the electron density at the boundary of the

Wigner–Seitz unit cell, n_{WS}, and a parameter Φ^*, which serves to describe the ionicity in metals. On the basis of this empirical model, de Boer et al (1988) compiled the binary phase diagrams, heat of formation, entropy of formation, etc for the transition metal alloys. In this way, a very modern collection of experimental thermodynamic data was created. For the physics of the planets, the knowledge of these composition temperature phase diagrams is by no means sufficient. After all, although they change by only small amounts for metallic alloys with moderately increasing pressures, this is by no means certain for pressures exceeding 100 GPa. The usual empirical models do not permit such a far-reaching extrapolation. Here, true first-principle calculations are more promising. Pseudopotentials are used for this purpose, and an inclusion into the calculation of tightly bound core states is thereby avoided. Many pseudopotentials are definitely dependent on the environment. Thus, eg in the case of iron, they differ from one another for small clusters and also for different alloys. For this reason one should use pseudopotentials which, through norm conservation, have an optimum transferability, and I shall base my considerations on the publications of Hamann et al (1979), Bachelet et al (1982), and Walzer (1991). In the latter work, one can find the considerations and formulae mentioned here summarised to explain the computer programs developed by the author.

Based on relativistic quantum mechanics, bare-ion pseudopotentials, $\hat{V}^{ion}_{l\pm 1/2}$ were derived through full-core atom calculations. These potentials are functions of r, the distance from the centre of the atom. The minima of these curves are each defined by one number triple

$$\begin{aligned} &r_{m0}, \upsilon_{m0}, e_{m0};\quad r_{m1}, \upsilon_{m1}, e_{m1};\quad r_{p1}, \upsilon_{p1}, e_{p1};\\ &r_{m2}, \upsilon_{m2}, e_{m2};\quad r_{p2}, \upsilon_{p2}, e_{p2};\quad r_{m3}, \upsilon_{m3}, e_{m3}; \end{aligned} \tag{13}$$

where r always denotes the pseudopotential radius of the minimum, υ is the potential, and e is the genuineness. For $e = 1$, (r, υ) is the first minimum of the pseudopotential–radius curve, which is reached coming from the infinite r. Both quantities are expressed in atomic units. The indices p and m denote, respectively, spin up and spin down; allowance for the spin–orbit effects has been made by the relativistic formulation of the theory. The indices 0, 1, 2, 3 denote the angular momentum quantum number l. If the minimum of the curve in question is reached only at $r = 0$, then $e = 0$. The pair of numbers (r, υ) then represents the point where simultaneously $d^2\upsilon/dr^2 > 0$ and where, coming from infinite r, the curvature k, becomes a maximum, with

$$k = \frac{d^2\upsilon}{dr^2}\left[1 + \left(\frac{d\upsilon}{dr}\right)^2\right]^{-3/2}. \tag{14}$$

4 Plotting of numerical results

The norm-conserving pseudopotentials for three chemical elements are shown in figure 2. With sodium no evidence of a relativistic splitting of the potentials can be observed. With molybdenum, it can already be seen that the coupling between each electron's orbital angular momentum and spin not only results in different energies and wave functions, but also in a splitting of the pseudopotentials. For the still heavier rhenium, this is even more pronounced. The characteristic pairs of numbers (r, υ), discussed above, are marked on the curves with short strokes. They were also determined with the use of a computer. In the following, 1 : 1 intermetallic compounds and alloys have been examined. In order to represent the first and second components, subscripts 1 and 2 have been added to the variables mentioned in equations (13). Simple mathematical combinations have been formed from these variables. These variables have been plotted and compared with measured values.

The experimental values from 1364 materials have been taken exclusively from the encyclopaedia of Villars and Calvert (1985); no value was excluded. This paper serves to represent, above all, the distribution of the melting temperatures of the intermetallic compounds and alloys. The radius melting temperature diagram (figure 3) shows distinct systematics. In the upper left area, the compounds of two transition metals (TT) are predominant; in the upper middle, the compounds of a simple and of a transition metal (ST) are predominant; at the bottom and on the lower right, only compounds and alloys of two simple metals (SS) each are present. Figure 4 shows the T_m systematics in a theoretically calculated radius–potential diagram. If, for instance, a 1:1 intermetallic compound, which has not yet been produced, is theoretically situated in the dense dark area to the left of the middle, very high melting temperatures are probable. The entire distribution of the points is also characteristic of other radius–potential diagrams.

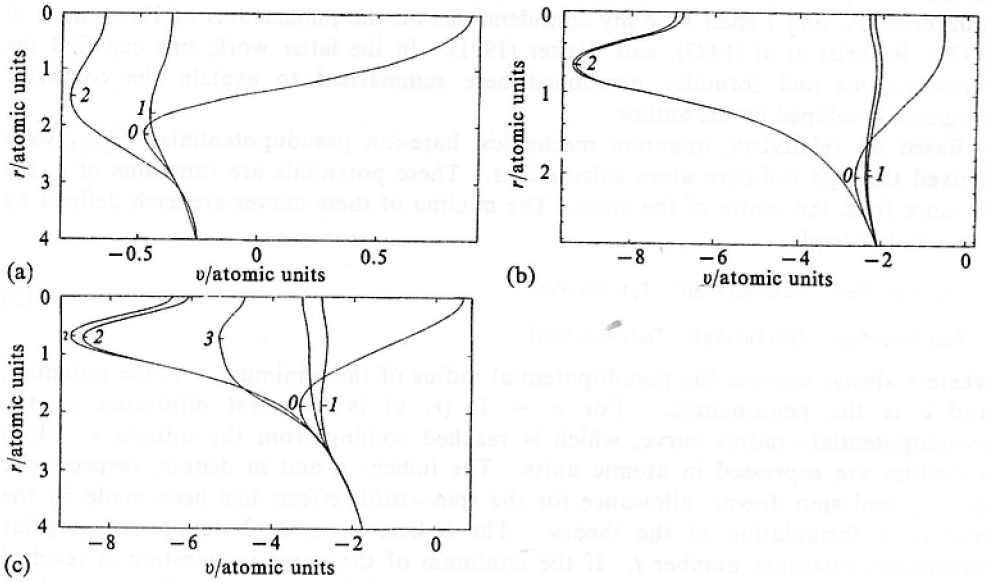

Figure 2. Pseudopotentials, υ, for (a) sodium, (b) molybdenum, and (c) rhenium. The distance, r, from the centre of the atom is plotted downwards. The numbers on the curves denote the angular momentum quantum number l.

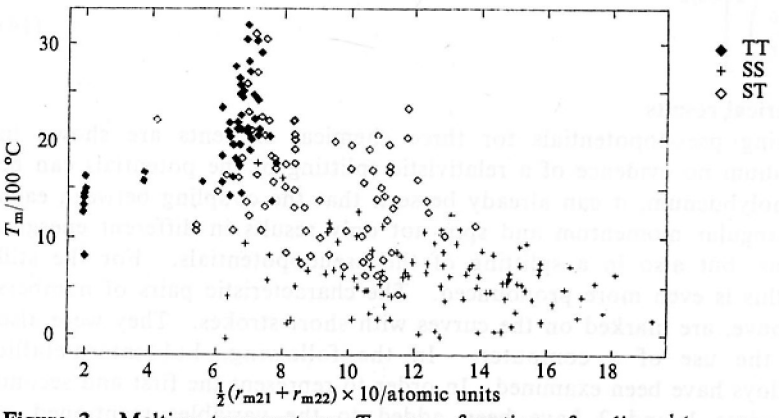

Figure 3. Melting temperature, T_m, as a function of radius, $\frac{1}{2}(r_{m21}+r_{m22})$, for $l = 2$. The symbols represent compounds and alloys of two transition metals (TT), of two simple metals (SS) and of simple and transition metals (ST), as shown.

For some diagrams, a simple function, F, has been used as one of the coordinates with $F = \frac{1}{2}(F_1 + F_2)$ and

$$F_i = 10\frac{s_p - 1}{18 - 1}(r_{m01} - 1)\upsilon_{m0i}, \tag{15}$$

where s_p denotes the column in the periodic table, and r_{m0i} and υ_{m0i} are expressed in atomic units. Figure 5 shows that a loose relationship exists between F and the melting temperature. This is similarly true of 1:1 compounds and alloys of two transition metals each (see figure 6 and table 1). Figure 7 shows that the relationship between F and the melting temperature is not quite as distinct, if all 1:1 compounds of all elements of the fourth, fifth and sixth period are permitted without lanthanides. The true significance of figure 7 becomes evident in figure 8, in which it is not the crystal lattice but the subdivision into types TT, ST, and SS, which governs the picture. One can easily recognise a triple division into areas in which only one type is predominant. Figure 9 shows a plot of two simple combinations of radii which can be calculated from the norm-conserving pseudopotentials, that is, ultimately, from the quantum theory. It can be seen that the melting temperatures of the intermetallic compounds and alloys exhibit distinct systematics, so that theoretical predictions are possible for materials which have not yet been produced.

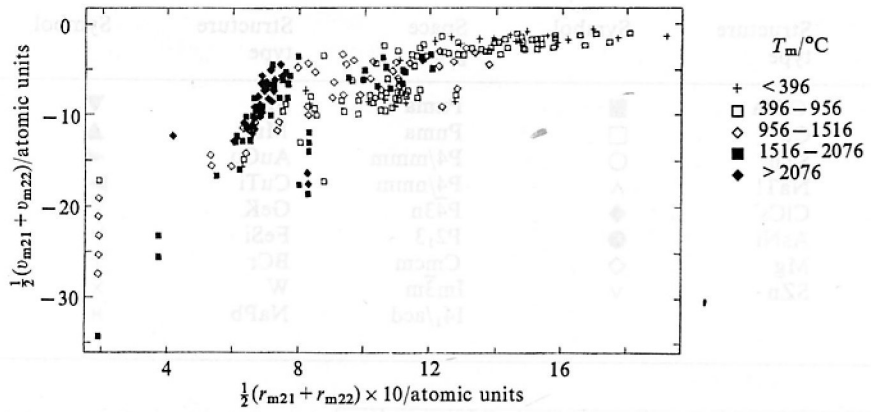

Figure 4. Potential, $\frac{1}{2}(\upsilon_{m21}+\upsilon_{m22})$, as a function of radius, $\frac{1}{2}(r_{m21}+r_{m22})$, for $l = 2$. Ranges of melting temperature, T_m, are indicated.

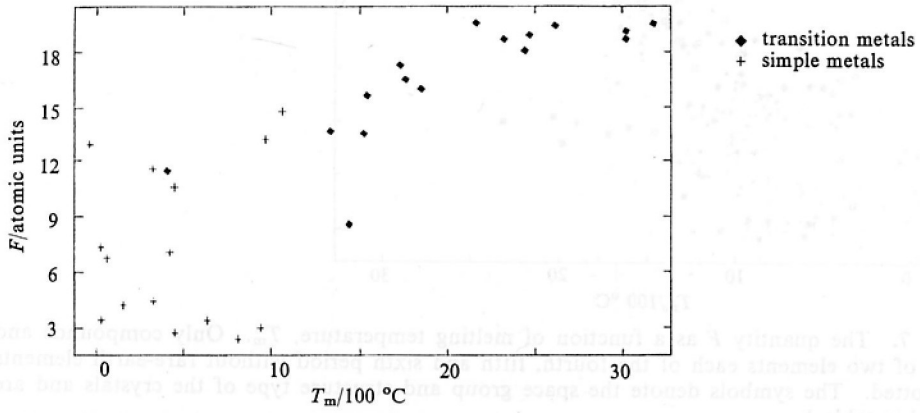

Figure 5. The quantity F as a function of melting temperature, T_m. Only the pure elements of the fourth, fifth and sixth period without rare-earth elements are shown.

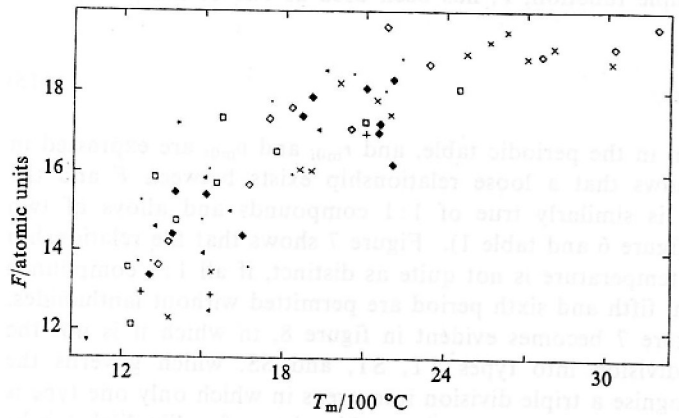

Figure 6. The quantity F as a function of melting temperature, T_m. All TT alloys and compounds are shown. The symbols denote the space group and structure type of the crystals and are defined in table 1.

Table 1. The assignment of symbols for the plots in which the symbols express the space group of the crystal lattice.

Space group	Structure type	Symbol	Space group	Structure type	Symbol
$Fm\bar{3}m$	ClNa	■	Pnma	BFe	▼
$Fm\bar{3}m$	Cu	□	Pnma	MnP	▲
$F\bar{4}3m$	SZn	○	P4/mmm	AuCu	◀
$Fd\bar{3}m$	NaTl	∧	P4/nmm	CuTi	▶
$Pm\bar{3}m$	ClCs	◆	$P\bar{4}3n$	GeK	<
$P6_3/mmc$	AsNi	●	$P2_13$	FeSi	>
$P6_3/mmc$	Mg	◇	Cmcm	BCr	+
$P6_3mc$	SZn	∨	$Im\bar{3}m$	W	×
			$I4_1/acd$	NaPb	*

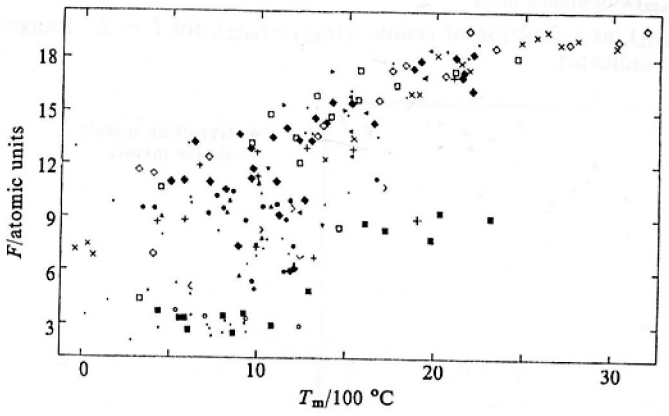

Figure 7. The quantity F as a function of melting temperature, T_m. Only compounds and alloys of two elements each of the fourth, fifth and sixth period without rare-earth elements are plotted. The symbols denote the space group and structure type of the crystals and are defined in table 1.

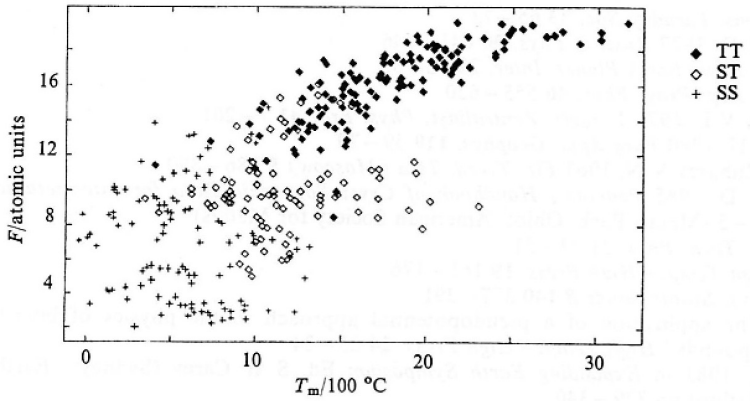

Figure 8. The quantity F as a function of melting temperature, T_m. The symbols represent compounds and alloys of two transition metals (TT), of one simple and one transition metal (ST), and of two simple metals (SS), as shown.

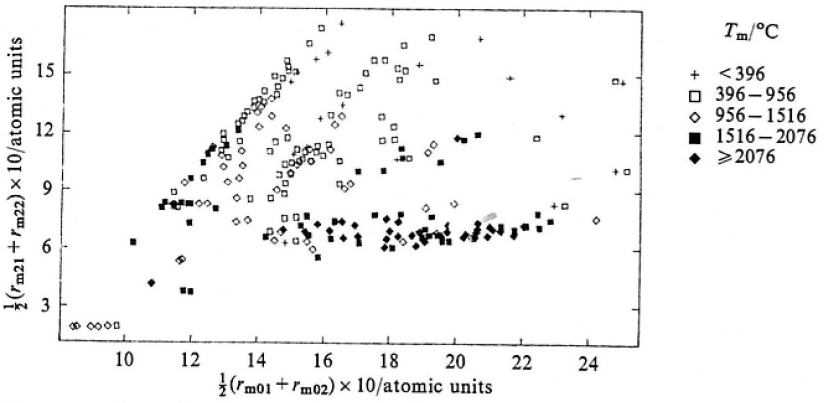

Figure 9. The radial quantity $\frac{1}{2}(r_{m21}+r_{m22})$ as a function of the radial quantity $\frac{1}{2}(r_{m01}+r_{m02})$. The ranges of melting temperature, T_m, are indicated.

5 Conclusions

Characteristic quantities have been derived from pseudopotentials with optimum transferability. In diagrams where these quantities or simple functions of the same have been plotted on the axes, one can observe a systematic distribution of the melting temperatures of intermetallic compounds and alloys. As a first step, the significance of the phase diagrams for the physics of the planetary cores has been considered.

References

Anderson O, 1989 *Deep-Earth Dialog* **3** 3–4
Bachelet G B, Hamann D R, Schlüter M, 1982 *Phys. Rev. B* **26** 4199–4228
Boehler R, 1986 *Geophys. Res. Lett.* **13** 1153–1156
Brown J M, McQueen R G, 1982 *Adv. Earth Planet. Sci.* **12** 611–623
de Boer F R, Boom R, Mattens W C M, Miedema A R, Niessen A K, 1988 *Cohesion in Metals–Transition Metal Alloys* (Amsterdam: North-Holland)
Gilvarry J J, 1956 *Phys. Rev.* **102** 308–316
Hamann D R, Schlüter M, Chiang C, 1979 *Phys. Rev. Lett.* **43** 1494–1497
Jacobs J A, 1987 *The Earth's Core*, 2nd edition (London: Academic Press)
Kubaschewski O, 1982 *Iron-Binary Phase Diagrams* (Berlin: Springer-Verlag)
Miedema A R, de Châtel P F, de Boer F R, 1980 *Physica B* **100** 1–28
Poirier J P, 1986 *Geophys. J. R. Astron. Soc.* **85** 315–328

Simon F E, 1937 *Trans. Faraday Soc.* **33** 65–73
Stacey F D, Irvine R D, 1977 *Aust. J. Phys.* **30** 641–646
Stevenson D J, 1980 *Phys. Earth Planet. Inter.* **22** 42–52
Stevenson D J, 1983 *Rep. Prog. Phys.* **46** 555–620
Ullmann W, Pan'kov V L, 1976 *Veroeff. Zentralinst. Phys. Erde* **41** 1–201
Ullmann W, Walzer U, 1980 *Pure Appl. Geophys.* **119** 59–79
Vashchenko V Ya, Zubarev V N, 1963 *Fiz. Tverd. Tela (Moscow)* **5** 886–890
Villars P, Calvert L D, 1985 *Pearson's Handbook of Crystallographic Data for Intermetallic Phases* volumes 1–3 (Metals Park, Ohio: American Society for Metals)
Walzer U, 1983 *Exp. Tech. Phys.* **31** 33–51
Walzer U, 1987a *High Temp.–High Press.* **19** 161–176
Walzer U, 1987b *Phys. Status Solidi B* **140** 377–391
Walzer U, 1991 "The application of a pseudopotential approach to the physics of binary intermetallic compounds" *High Temp.–High Press.* **24** 23–34
Walzer U, Maaz R, 1983 in *Expanding Earth Symposium* Ed. S W Carey (Sydney: Earth Resources Foundation) pp 329–340
Walzer U, Ullmann W, Pan'kov V L, 1979 *Phys. Earth Planet. Inter.* **18** 1–12
Williams Q, Jeanloz R, Bass J, Svendsen B, Ahrens T J, 1987 *Science* **236** 181–182

© 1992 a Pion publication printed in Great Britain